Status of an extreme adaptive optics testbench using a self-referenced Mach-Zehnder wavefront sensor

M. Loupias, M. Langlois, E. Thiébaut, M. Tallon, J. Leger

Status of an extreme adaptive optics testbench using a self-referenced Mach-Zehnder wavefront sensor

M. Loupias*[a], M. Langlois[a], E. Thiébaut[a], M. Tallon[a], J. Leger[a]
[a]Univ Lyon, Univ Lyon1, Ens de Lyon, CNRS, Centre de Recherche Astrophysique de Lyon UMR5574, F-69230, Saint-Genis-Laval, France

ABSTRACT

Extreme adaptive optics (XAO) systems have severe difficulties to meet the following high contrast requirements: high speed (>1kHz) and high accuracy (~ 10 nm) at 5-10 cm spatial scale. An innovative high order adaptive optics system using a self-referenced Mach-Zehnder wavefront sensor has been proposed to counteract these limitations. This wavefront sensor estimates the phase by measuring directly intensity differences between two outputs, but has a limited dynamical range. In this paper, we report on our latest results with the XAO testbed in operation in our lab, and dedicated to high contrast imaging with 30m-class telescopes. A woofer-tweeter architecture is used in order to deliver the required high Strehl ratio (>95%). We present our latest laboratory results, including fine calibration and closed loop performance. This work is carried out in synergy with the validation of fast iterative wavefront reconstruction algorithms, and the optimal treatment of phase ambiguities in order to mitigate the dynamical range limitation of such a wavefront sensor.

Keywords: Wavefront sensing, Mach-Zehnder interferometer, deformable mirror, spatial light modulator, optimal control, fractal iterative method

1. INTRODUCTION

Extreme adaptive optics (XAO) is a key challenge for Extremely Large Telescopes (ELT). From the large range of spatial frequencies to correct with high accuracy, to the speed of the control loop, including the co-phasing of mirrors segments, all these requirements need to go one step forward. At CRAL (Centre de Recherche Astrophysique de Lyon), we have developed an experimental bench to test, analyse, and propose alternative solutions related to XAO and high contrast instrumentation. Our high order adaptive optics system uses a self-referenced Mach Zehnder sensor. With respect to classical Shack Hartmann wavefront sensor (WFS), the Mach-Zehnder WFS allows a higher spatial resolution without noise propagation from the reconstruction, and under given conditions can deliver nanometer accuracy. Hence high order frequencies artefacts introduced by the telescope spider and segmented pupil, have negligible impact on the phase measurements with this type of WFS by opposition to Shack-Hartman or Pyramid wavefront sensors. Nevertheless the Mach-Zehnder WFS suffers from some drawbacks like its small dynamical range, and its alignment sensitivity to tip-tilt, that needs to be addressed to make it a performant sensor for extreme adaptive optics system. The optimal analysis of the phase ambiguities and the use of fast iterative wavefront reconstruction algorithms are key developments carried out by our team on the XAO test bench.

In this paper, we present the setup and calibration of the experimental test bench, dedicated to the study of XAO for 30m-class ELTs. The Mach-Zehnder Wavefront Sensor (MZWFS) principle and the demanding performances of Adaptive Optics for ELT's are detailed and compared in section 3 and 2. In Section 4, we describe the characterization of the Deformable Mirror (DM) phase corrector, whereas the calibration of the Spatial Light Modulator (SLM) is the topic of section 5. In the section 6, we discuss the implementation of both correctors in closed loop with the MZWFS.

*magali.loupias@univ-lyon1.fr; phone (33)478868398

2. SET-UP PERFORMANCES

Our set-up can make use of different light sources: either a He-Ne laser or a broadband white laser covering a 500 to 900 nm spectral range. Each light source is spatially filtered at the focus of a lens, in order to build a clean wavefront collimated beam. A diaphragm in the collimated beam, represents the simulated telescope pupil which can be disturbed by a rotating phase screen that mimics real atmospheric turbulence. This perturbated pupil is reimaged several times in the setup through 2f optical systems. The first reimaged pupil is on the Spatial Light Modulator (SLM), the second one is on the Deformable Mirror (DM) and finally the pupil is reimaged on the Camera, on which, the two Mach-Zehnder outputs are imaged side by side. All these elements are represented on Figure 1.

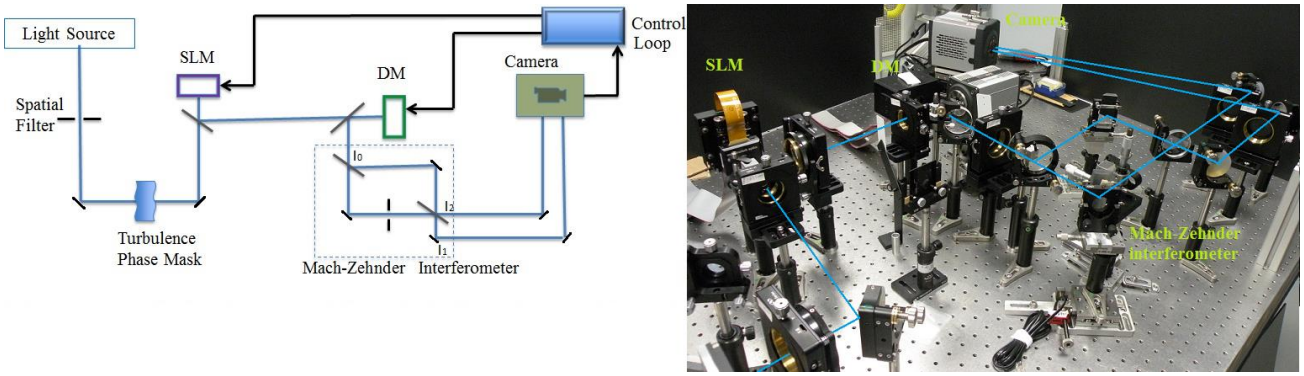

Figure 1: Left :Optical scheme of the XAO setup. Right: XAO test bench picture.

The pupils diameters are optimized separately to each plane: on the SLM which is a 512x512 pixels liquid crystal, on the DM which is 12x12 actuators membrane, and on the Mach-Zehnder camera where both pupils are imaged with more than 1200 pixels in diameter. Table 1, shows a performance comparison of our setup with the one expected for 30m-class ELTs XAO. Our experimental bench achieves the spatial resolution we need to achieve for the woofer or the tweeter corrector since ELTs XAO will require more than 20000 actuators[4]. The wavefront correction dynamical range is limited to one wavelength for our Spatial Light Modulator whereas the Deformable Mirror is able to produce 4 to 5λ peak to valley amplitude deformation. This woofer-tweeter architecture aims at increasing the Strehl ratio up to 95% while dealing with large wavefront amplitudes from the atmospheric turbulence phase screen. The control of all the bench elements is performed via a Linux workstation, using Yorick language. One important goal is to test the different control algorithms to reach the high control frequency required.

System overview		
	XAO Setup scale	ELT scale
Mach-Zehnder wavefront sensor		
Pupil spatial resolution	1200 pixels	3.5cm
Wavefront detection accuracy	~a few nanometer	
Deformable Mirror corrector: woofer		
Pupil spatial resolution	12x12 actuators	2.9m
Wavefront correction dynamic	~6 microns PTV	
Spatial Light Modulator corrector: tweeter		
Pupil spatial resolution	512x512 pixels	7 cm
Wavefront correction accuracy	~4 nanometer	
Turbulence phase screen		
Pupil spatial resolution	3000 pixels on diameter	1cm
Wavefront accuracy	~15 nanometer	
Control Loop		
Control frequency	~100Hz	~1kHZ

Table 1: System overview and comparison with ELT scale requirements

3. MACH-ZEHNDER INTERFEROMETER

The Mach-Zehnder interferometer[3] is a WFS measuring phase variation directly in a pupil plane. The interferometer has two arms created by two beam splitters and two mirrors. A lens located before the Mach Zehnder produces a focal plane inside each arm. A pinhole is positioned at the focal plane of one arm and spatially filters the beam to provide a reference wavefront. The two outputs of the Mach-Zehnder produce an image of the interference between the reference wavefront and the aberrated wavefront coming from the telescope pupil. One output is called the symmetric output because each beam undergoes one reflection and one transmission by a beam splitter, whereas the anti-symmetric output is produced by one beam transmitted twice and the other one reflected twice. The analytical expression of the two outputs of a Mach-Zehnder assuming the two beam splitters are non-absorbing, identical with a transmission coefficient T, are:

For the symmetric output $I_1 = 2RTI_0\,(1 + \cos k\Delta)$
For the anti- symmetric output $I_2 = I_0 - 2RTI_0\,(1 + \cos k\Delta)$
with T=1-R, I_0 the input intensity of the beam entering the MZ, $k=2\pi/\lambda$, λ being the wavelength of the light and Δ the path difference between the two arms.
With equally balanced arms R=T=1/2 we can remove the continuous part using the difference of the two ouputs.
$S = I_1 - I_2 = I_0 \cos k\Delta$

Developing this equation[5], the impact of the size of the pinhole can be assessed (in one dimension). A classical implementation of the Mach-Zehnder uses a pinhole diameter smaller than the Airy disk and a phase offset of $\pi/2$ using a $\lambda/4$ plate on one arm, to create a signal directly proportional to the phase for small phase variations.
$S(x) = \frac{2D\sqrt{St}}{l\sqrt{\pi}}\sin(\varphi(x)) \approx \frac{2D\sqrt{St}}{l\sqrt{\pi}}\varphi(x)$,with D the pupil diameter, St the Strehl ratio, $l=\lambda/0.6\pi a$, a being the pinhole width, and $\varphi(x)$ a one dimensional phase variation.

The wavefront error signal retrieval used in this article is a simple combination of the two outputs of the Mach-Zehnder using the following equation : $E = (I_1 - I_2)/(I_1 + I_2) = \cos k\Delta$.
To estimate the wavefront error, a position calibration of the 2 pupils recorded on the camera has been implemented. This is achieved by using a target positioned on the input pupil, and by creating an image with only one arm of the Mach Zehnder i.e. an image without interference is recorded. Each pupil is sampled with ~1200 pixels on its diameter. A matching program using the affine scale invariant matching method[7] has been used. It matches key points from one pupil to the second one in order to to retrieve the translation, rotation and magnification necessary to fit one pupil to the other. This method allows to compute phase measurements using both pupils within the pixel accuracy.

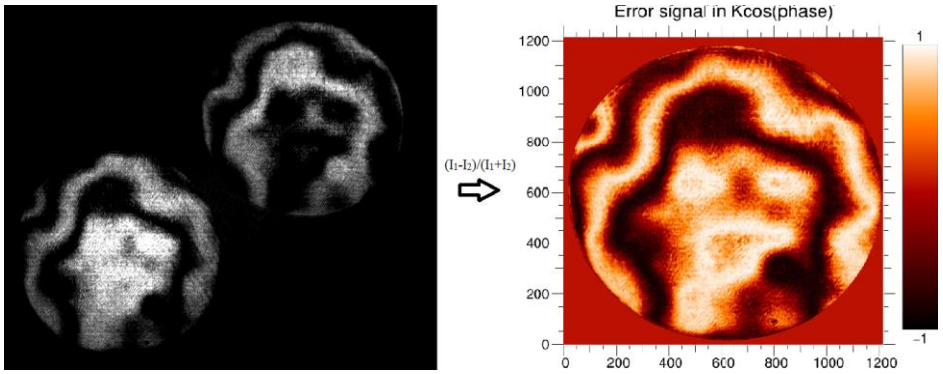

Figure 2: Computation of the error signal: the left image is the raw image of the two Mach-Zehnder outputs from the camera. The right image shows the the wavefront measurement computed from these two outputs.

4. DEFORMABLE MIRROR CALIBRATION

The woofer wavefront corrector is a Boston Micromachine continuous membrane deformable mirror (DM). This microelectromechanical system (MEMs) has 140 actuators on a 12x12 grid, for a 4.4×4.4 mm clear aperture. The inter-actuator spacing is 400 μm. This DM exhibits a maximum stroke of 3.5 microns. This component has been calibrated first using a ZYGO interferometer[6] and we report here on the second step of the calibrations using directly the Mach Zehnder WFS.

Using the Mach Zehnder WFS, the first step has been to calibrate the DM actuators positions using the Mach-Zehnder error signal. To do so a few actuators on the diameter of our pupil are pushed, and the grid of actuators is finely adjusted to fit these actuators.

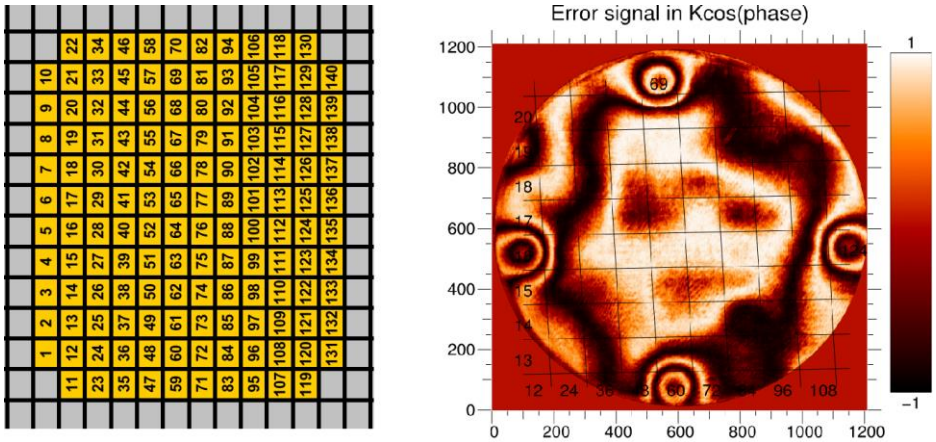

Figure 3: Calibration of the DM: Left, grid of numbered actuators, Right, four known actuators have been pushed up to locate the grid of actuators on the error signal from the Mach-Zehnder .

As it can be seen in Figure 3, the supplier flat map exhibits some structure when recorded with the MZWFS accuracy. A flat map has been manually created to flatten the central zone of the DM and to decrease this structure. It becomes then possible to evaluate the influence function of the central actuators. Figure 4, shows the wavefront measured when pushing up the DM actuator 64.

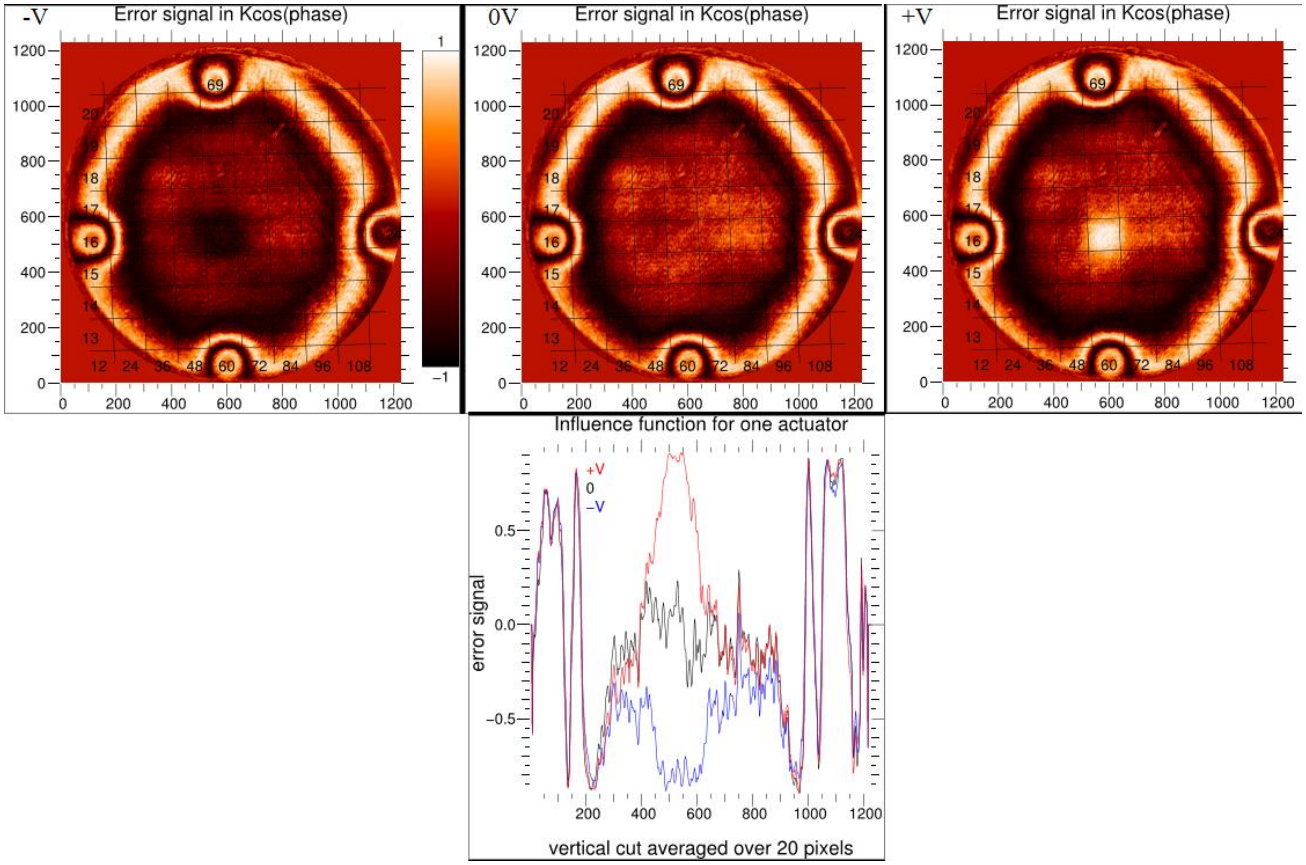

Figure 4: Mach-Zehnder error signal obtained from the influence function measurements on the actuator 64: Left the actuator is fed with –V, Middle: the actuator is at rest, Right: the actuator is fed with +V= 9.15V~0.3λ , Bottom: Vertical profile of the 3 images averaged horizontally over 20 pixel.

The error signal profile (Figure 4) shows on both ends the wrapping of the signal for the actuators 60 and 69. These actuators have been lifted to ~1.3microns~2λ. They are used as a phase reference to insure that no piston is introduced in the measurement. One can see that actuators separated by 3 actuators distance do not influence each other. For the actuator 64 in the central zone, the phase shift induced is consistent with the supplier phase response calibration. Nevertheless the wrapping of the error signal is still an issue when reaching the +/- π/2 limit. An unwrapping method is still under investigation to cope with this limitation, making some hypothesis on the local curvature of the phase.

5. SPATIAL LIGHT MODULATOR CALIBRATION

The wavefront tweeter corrector is a Meadowlark (formerly Boulder Nonlinear Systems i.e. BNS) liquid crystal spatial light modulator (SLM), 512×512 pixels on a 7.68 mm square grid. The XY nematic liquid crystal SLM is optimized to produce a full wave of phase stroke upon reflection at 632nm. It creates phase only modulation on a polarized input beam. As for the DM, the SLM has been first calibrated on the ZYGO interferometer (see Figure 5). The SLM is addressed with a linear ramp of modulation in one direction to cover the full 2π phase variation. Each pixel of the SLM

can be addressed from 0 to 255 in grey level. Below a threshold of 100 in grey level the SLM does not respond uniformly from one pixel to another. The amplitude calibration of its response has been done above this threshold.

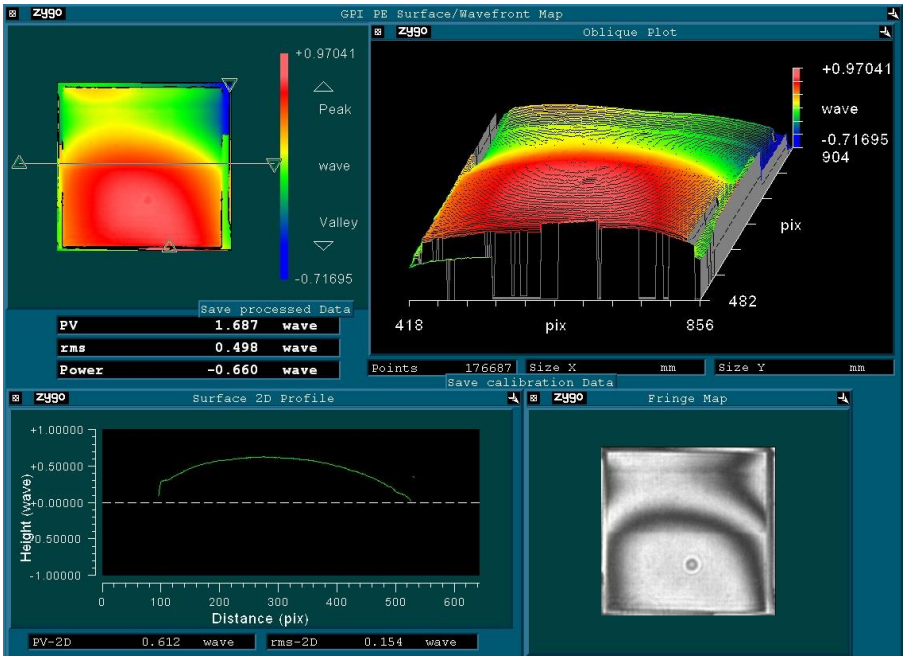

Figure 5(a): Calibration of the SLM loaded with a phase ramp on the vertical direction, using the ZYGO interferometer. Top pictures: 2D and 3D representation of the reconstructed phase, Bottom left: Cut in the horizontal direction of the phase map. Bottom right: the interference pattern recorded on the ZYGO.

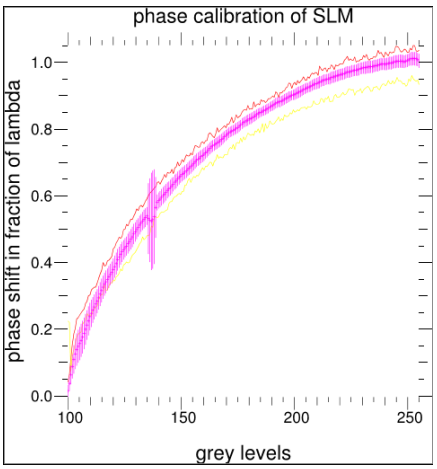

Figure 5(b): Analysis of the SLM calibration: response of the pixels to the grey level ramp, average and standard deviation**.** One can see on all the pictures an artefact due to a dust in the ZYGO which is not present in the XAO bench.

A further step in the calibration will be to build a pixel to pixel response of the SLM to improve the performance, and potentially use the SLM over the 2π phase correction if necessary. The SLM has also been calibrated directly on the Mach Zehnder. Figure 6, shows the π phase shift induced by the SLM loaded with a map included 16 dephased squares over the pupil on top of the non dephased background .

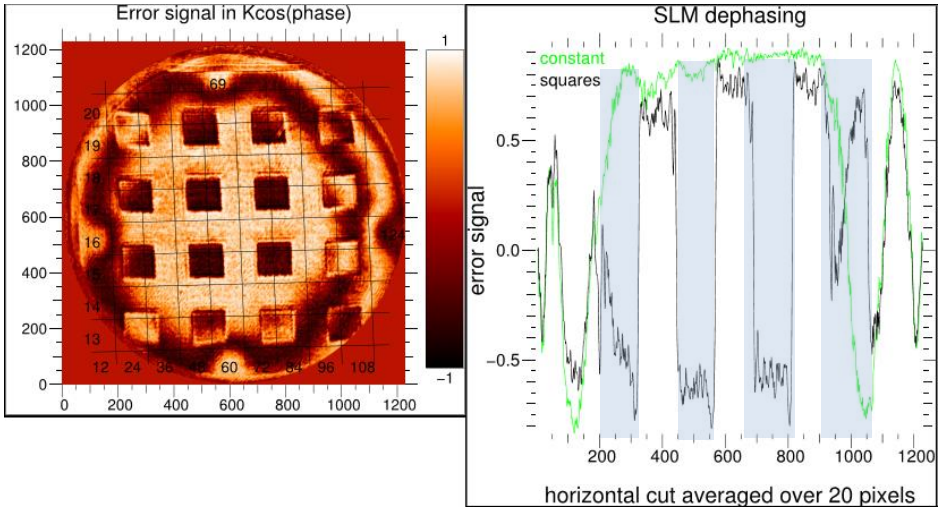

Figure 5(a): The SLM is loaded with a map containing 16 squares shifted in phase by π. Right: Error signal recorded by the Mach-Zehnder, Left: Profile of the error signal along the horizontal direction averaged over 20 pixels (from 670 to 690 in y coordinate). The light color curve is the done with the SLM loaded with a constant map, whereas the black color line is obtained with the MZWFS with the SLM loaded with 16 squares producing λ/2 shift. The 4 zones dephased of π are highlighted.

In order to estimate the phase residuals of the SLM correction, we calculate the difference of the arccosine of the error signals between the 2 curves, with the SLM loaded either with a constant map or with a map with squares. A binning by 2 has been applied to rescale to SLM pixel size to a more resonnable measurement spatial scale. The standard deviation of a 30 x30 pixels zone (corresponding to a square) is 0.12π, i.e. 0.06λ. This rough estimation of the closed loop accuracy is already very promising knowing that there is still room for improvement in signal processing: by averaging few frames, removing dark signal etc…. As for the DM, the registration of the SLM on the Mach-Zehnder WFS has been done using a few points over the pupil to match and rescale properly the WFS and SLM pupils.

6. IMPLEMENTATION OF BOTH CORRECTORS

Both active correctors being characterized, we have fed them with the Mach Zehnder error measurements to estimate the efficiency of the correction. We have first chosen a phase map produced by the SLM, and corrected by the DM. The Mach-Zehnder interferometer is very sensitive to tip-tilt errors. Actually the pinhole positioned in the focal plane of the reference arm is of the order of magnitude of the Airy disk. A tilt of one milliradian of the wavefront would divide the light flux passing through the reference arm by more than two and reduce significantly the visibility of the interference pattern. Hence before any correction by the DM, the first Zernike modes (piston and tilts) are removed. The correction is effective only for the central zone using 5*5 DM actuators. Eventhough this is doomed to failure to correct high spatial frequencies wavefront errors induced by the SLM with the low spatial frequencies correction of the DM, this allows to check the functionality of the correction, the behavior of the corrector as well as the wavefront error signal.

On Figure 7 one can clearly see the influence function of the actuators of the DM. Eventhough neglected in this first step, the overall interaction matrix remains to be built to take into account the influence of the neighbouring actuators to better estimate the correction to apply.

The same correction principle has been implemented by exchanging the wavefront correctors. This time, we introduced a phase error with the DM and we correct it with the SLM (see Figure 8). In this case we also have been only correcting the central zone (using ~200 x 200 pixels of the SLM). The result obtained in only one iteration is already very accurate but the phase calibration of the SLM can be improved to take into account pixel to pixel phase response variations.

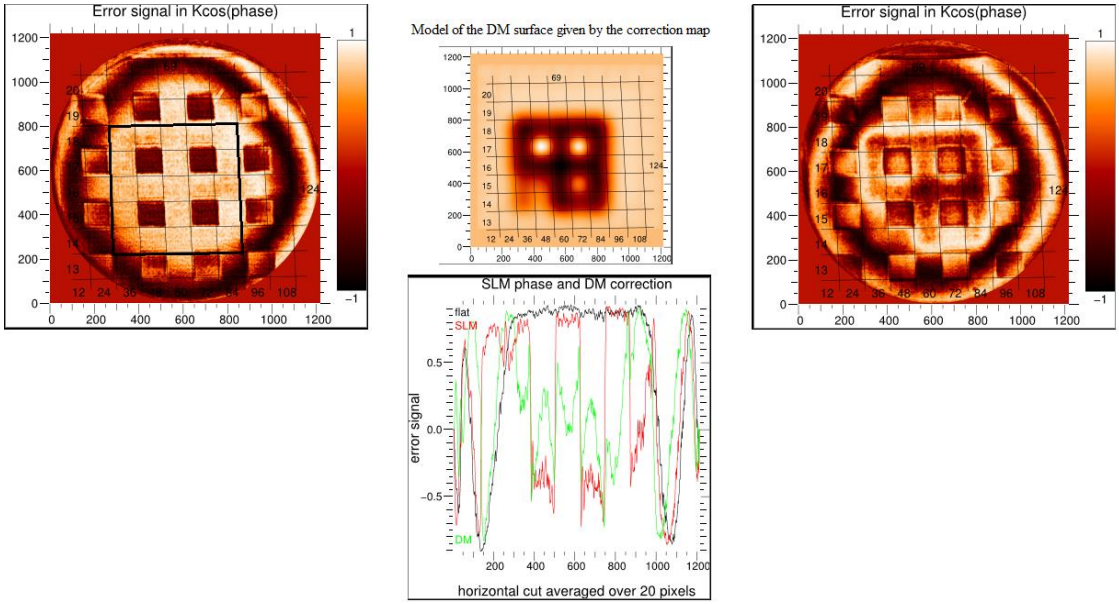

Figure 7: Top left is the error signal produced by the SLM loaded with squares (as previously), the thick surrounded square zone shows the zone of interest where the DM correction will be applied. Top middle shows the model of the correction sent on the DM, simply using a Gaussian influence function (the standard deviation of which is equal to 0.5 actuator size) for each actuator. Top left shows the corrected image by the DM. Bottom plot shows a cut of the different correction steps: the "flat "black solid line shows the Mach-Zehnder error signal (in 1 D) without any perturbation, "SLM" red solid line shows the error induced by the SLM loaded with squares, "DM" green solid line shows the wavefront residual error measured after the correction by the DM.

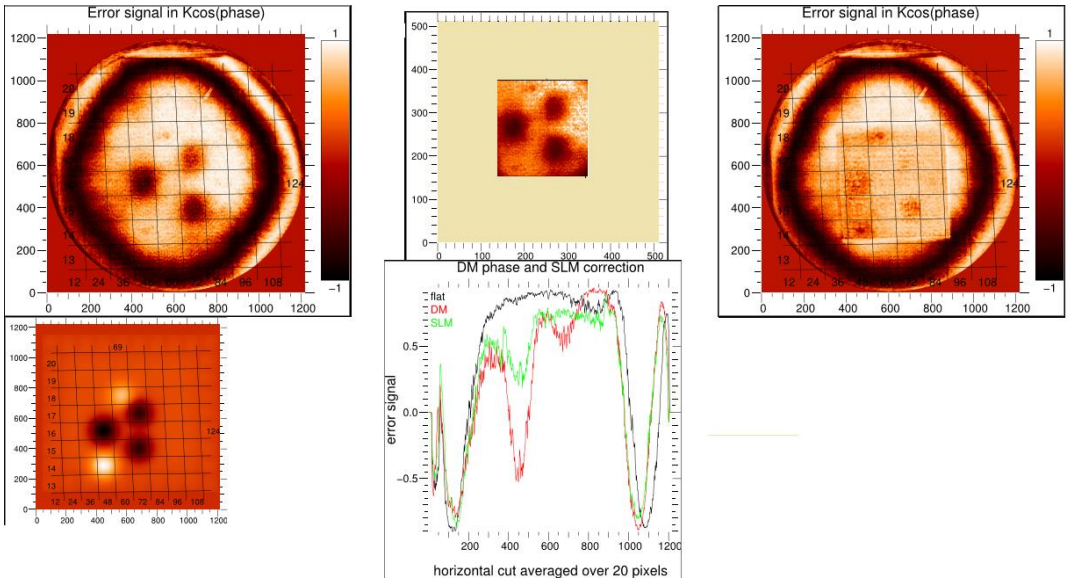

Figure 8: Bottom left image shows the model of the wavefront error sent by the DM, Top Left image shows the wavefront error measured by the Mach-Zehnder produced by the initial DM wavefront error, Top middle image shows the central zone correction wavefront sent to the SLM, Bottom left image shows the Mach-Zehnder wavefront error signal obtained after the SLM correction. The bottom middle figure shows the profiles of the Mach –Zehnder wavefront error signal at the different steps: the "flat " curve is the Mach-Zehnder error signal without any perturbation, "DM" curve is the error induced by the DM loaded with the error map, "SLM" is the error signal after correction by the SLM.

These first results validate the use of a Mach-Zehnder to achieve very high strehl ratio (90% Strehl ratio has been already obtained on our test bench). We foresee several improvements to make the measurements more accurate and to improve the robustness of this WFS in order to unable sky use: We plan to (1) implement the inverse approach to estimate more accuratly the wavefront error signal in order to minimize the residual errors, (2) develop an unwrapping technique adapted to the Mach-Zehnder signal. We also plan to improve the pupil position registration for both SLM and DM by including rotation. We will produce a pixel to pixel phase calibration for the SLM, and an interaction matrix for the DM actuators. We also plan to upgrade our light source with a less coherent one like the broadband laser which will reduce the injection of high order wavefront fluctuations from interferences. Last but not least we plan to test the benefit of the fractal iterative method (FRiM)[9] , a fast iterative algorithm for minimum variance wavefront reconstruction and control.

7. CONCLUSION AND PERSPECTIVES

We have built an experimental XAO test bench dedicated to the ELTs and equipped with a Mach-Zehnder WFS to accurately estimate and correct, in closed loop, the wavefront phase errors at small spatial scale, using a woofer tweeter phase correctors architecture (DM and SLM).. The phase correctors were characterized using a Zygo interferometer, and directly on the XAO bench with Mach Zehnder WFS. A simple but efficient method was used to estimate the wavefront error signal. First results obtained with the MZWFS, using monochromatic light already show an improvement of the Strehl ratio up to 90% when using artificial static phase maps. The next steps are the use of adapted control algorithms like Frim in real time among with the use of polychromatic light to reduce fringe effects.

ACKNOWLEDGEMENT

The authors are grateful to the LABEX Lyon Institute of Origins (ANR-10-LABX-0066) of the Université de Lyon for its financial support within the program "Investissements d'Avenir" (ANR-11-IDEX-0007) of the French government operated by the National Research Agency (ANR).

REFERENCES

[1] Fusco, T., Sauvage, J.-F., Petit, C., et al., "Final performance and lesson-learned of SAXO, the VLT-SPHERE eXtreme AO: from early design to on-sky results," *Proc. SPIE* **9148**, 91481U-15 (2014).
[2] Angel, J. R. P., "Ground-based imaging of extrasolar planets using adaptive optics," *Nature* **368**, 203 (1994).
[3] Langlois, M., Angel, J. R. P., Lloyd-Hart, M., et al., "High Order, Reconstructor-Free Adaptive Optics for 6-8 meter class Telescopes," *Proc. Beyond Conv. AO* **58**, 113-120 (2001).
[4] Langlois, M., Pasanau, C., Leroux, B., et al., "Progress with extreme adaptive optics test bench for ELT at LAM," *Proc. SPIE* **7015**, 701544 (2008).
[5] Yaitskova N., Dolhen K., Dierickx P., Montoya L., "Mach-Zehnder interferometer for piston and tip-tilt sensing in segmented telescopes: theory and analytical treatment" *J. Opt. Soc. Am. A* **22**, 1093–1105 (2005)
[6] Delacroix, C., Langlois, M., Loupias, M., et al., "Development of an ELT XAO testbed using a Mach-Zehnder wavefront sensor: calibration of the deformable mirror," *Proc. SPIE* **9617**, 96170G-9 (2015).
[7] G. Yu, J-M Morel, "ASIFT: An algorithm for Fully Affine Invariant Comparison", *Image Processing On Line*, **1** (2011) http://dx.doi.org/10.5201/ipol.2011.my-asift
[8] Lane, R. G., and Tallon, M., "Wave-front reconstruction using a Shack-Hartmann sensor," *Appl. Opt.* **31**, 6902-6908 (1992).
[9] Tallon, M., Tallon-Bosc, I., Béchet, C., et al., "Fractal iterative method for fast atmospheric tomography on extremely large telescopes," *Proc. SPIE* **7736**, 77360X (2010).